C.P. No. 1036

MINISTRY OF TECHNOLOGY

AERONAUTICAL RESEARCH COUNCIL

CURREN J PAPERS

On the Prediction of Laminarisation

BY

B. E launder and W. P. Jones

Department of Mechanical Engineering,

Imperial College, London.

LONDON: HER MAJESTY'S STATIONERY OFFICE

1969

Price 6s 6d net

C. P. No. 1036*

February, 1968

ON THE PREDICTION OF LAMINARISATION

by

B. E. Launder+ and W. P. Jones‡
Department of Mechanical Engineering,
Imperial College, London.

SUMMARY

In rapid accelerations it is known that an originally turbulent boundary layer may undergo a partial or complete decay to laminar; a phenomenon known as laminarisation. The report distinguishes between 'moderate' and 'severe' accelerations. For the former, the sublayer of the boundary layer undergoes considerable change in structure but the boundary layer remains essentially turbulent. For the latter, a complete degeneration to laminar flow will take place if the acceleration continue.3 over a sufficient distance.

Two simple models have been proposed for the variation of turbulent shear stress, according to whether the acceleration is 'moderato' or 'severe'. These models have been incorporated into the finite difference prediction procedure of Patankar and Spalding and comparison made with a limited number of experiments. Agreement with experiment is reasonably good and progress to date has been sufficiently encouraging to suggest that the accurate prediction of laminarisation is now an attainable objective.

+Lecturer in Mechanical Engineering-

‡Research Student, Mechanical Engineering.

*Replaces A.R.C.30 067

1. Introduction

1.1 The occurrence of laminarisation

When a turbulent boundary layer undergoes a severe acceleration it may revert partially or completely to laminar. A variety of labels have been given on the phenomenon; in this paper it is termed 'laminarisation'. Over the last dozen years a number of workers have observed laminarisation! (Refs.1 - 11). Of these, Refs.9, 10 and 11 contain the most complete experimental examinations of the problem.

Figs.1 and 2 illustrate some of the effects of laminarisation on the gross features of the boundary layer. Fig.1 shows the variation of the shape factor, Ii, along a plate in which the free-stream dynamic pressure is increased by a factor of 6 over a length of 6inches. The shape factor is a convenient parameter with which to distinguish between a turbulent and a laminar boundary layer. In zero pressure gradient H is equal to about 2.6for a laminar boundary layer, while, in turbulent flow, it takes values between about 1.6 and 1.2 depending on Reynolds number. For both laminar and turbulent flow, an acceleration causes the shape factor to decrease from its flat-plate value.

For the boundary-layer development shown in Fig.1, the shape factor is about 1.6 upstream of the contraction and initially decreases along the nozzle. However, H then begins to rise sharply and reaches a value of about 1.8 at the end of the contraction. The shape factor then continues to increase as the boundary layer continues its development in near-zero pressure gradient. The mean velocity profiles at three stations are shown in inset on Fig.1. The change in the profile shape from turbulent upstream flow to that of a laminar boundary layer downstream is clearly evident.

The above example is one of a 'fully-laminarised' boundary layer where the acceleration was sufficiently rapid and occurred over a sufficient length for the reversion to a laminar boundary layer to be virtually complete. When the pressure gradient was removed, the boundary layer continued to develop some distance downstream as though it were laminar. As a second example of laminarisation, Fig.2 shows some surface heat-transfer data of Filetti (Ref.7) quoted by Moretti and Kays (Ref.10). The test plate is maintained at a nearly uniform temperature from 2 ft along the test plate and an acceleration is imposed at about 4 ft from the leading edge. The Stanton number falls sharply in the accelerated region but quickly rises again when the pressure gradient is removed. Here, then, the boundary layer undergoes only partial laminarisation and, with the removal of the pressure gradient, the original turbulence structure is quickly re-established.

Figs.1 and 2 also show the variation of the parameter K (defined as $\frac{\nu}{U_G^2}\frac{dU_G}{dx}$) through each of the test sections. Experiments have shown that when K exceeds a value of about 2×10^{-6}, laminarisation effects will become significant. In each of the quoted tests K exceeded this value. Theoretical consideration (Ref.11) suggests that the parameter L, $(K.c_f^{-6/5})$, rather than K, should determine the onset end degree of laminarisation and we shall make use of this parameter later. In most situations of practical interest, however, c_f will lie between about 0.003 and 0.005, so the value of K alone provides a reasonable indication of whether or not laminarisation till occur.

The occurrence of lsminarisation is probably of greatest importance in the design of rocket nozzles. Parkinson (Ref.13) has found from an examination of considerable heat-transfer data that for a region upstream of the throat, conventional turbulent boundary-layer theories predict Stanton numbers up to 100% higher than measured values.

Strong/

Strong accelerations are also present in the flow over gas turbine blades, though it would seem rather unlikely that laminarisation would occur in such geometries. The maximum free-stream acceleration occurs at the stagnation point (where the boundary layer is laminar) and diminishes towards the trading edge. One would thus expect that when the boundary layer became turbulent it would remain so.

Zaric (Ref.8) appears to have detected laminarisation in what would, at first glance, seem an unsuitable environment; namely, flow through a roughened. passage. The roughened surface was of a continuous symmetric saw-tooth form with apex angle of 14-P. The flow near the rough surface was alternatively accelerated and retarded due to the profile of the rough surface. Towards the end of each accelerated region the local surface Stanton number dropped significantly and the measured mean velocity profiles were similar in shape to those shown in Fig.1.

In the above example, the reversion of the boundary layer towards laminar is an undesirable effect since a surface is generally roughened to promote the transfer of heat. Another unsought-for effect can occur when a rapid acceleration is followed by an adverse pressure gradient; for then, if laminarisation takes place, boundary layer separation may occur at a much lower pressure coefficient than for a turbulent boundary layer (Ref.9). Such a situation might arise in flow normal to a row of closely packed tubes.

Whether or not laminarisation is a desirable feature in any particular situation, however, the need to develop a reliable means of boundary-layer prediction in highly-accelerated flows is obvious. It is a theme which is taken up in Section 2 of this report.

1.2 Sink-flow turbulent boundary layers

The similar turbulent boundary layers which develop between plane converging walls are of particular importance in the study of laminarisation. For these flows, the parameter K is invariant with x and the two-dimensional partial-differential momentum and continuity equations reduce to a second-order ordinary differential equation in terms of a similarity variable proportional to $(\frac{U_G y}{\nu})$. It is readily demonstrated that for these boundary layers the local Reynolds number and skin friction coefficient are each constant throughout the flow. Theoretical solutions to these constant-k boundary layers may be obtained by using, for example, a mixing-length hypothesis to relate the Reynolds shear stress to the local mean velocity gradient; the solutions would be computed either by numerical solution of the ordinary differential equation of motion or by a finite-difference procedure.

Attention will be turned to these theoretical solutions in Section 2; here our purpose is to consider the implications of experimental investigation . A recent study (Ref. 12) has succeeded in establishing similar sink-flow turbulent boundary layers at three values of K; namely 0.7×10^{-6}, 1.3×10^{-6} and 3×10^{-6}. As the value of K was successively increased, the mean velocity profiles exhibited a progressive change towards those of a laminar boundary layer. Even at the highest value of K, however, there was a large and self-preserving turbulence distribution across the boundary layer. These findings are Important for they show that, over a significant range of accelerations, while definite changes in the turbulence structure near the wall takes place, the boundary layers remain essentially turbulent. Thus, only in the most general sense should laminarisation be thou&t of as 'the opposite of natural transition'.

The findings confirm Schraub and Kline's (11) visual studies of accelerated boundary layers. In the sublayer, they found that the sinuous low-momentum streaks, which are a characteristic of turbulent boundary layers, did not suddenly cease to form above a certain value of K but, instead, gradually disappeared as the acceleration parameter was increased.

An encouraging inference from these results is that, for 'moderate' accelerations, (for values of K up to about 3×10^{-6}) existing turbulent boundary layer theories should, with only slight modifications, be capable of predicting the effects of laminarisation. That is to say, we might hope to predict completely the Stanton number behaviour shown in Fig.2; however, the virtually complete reversion to laminar of the boundary layers of Fig.1 would be outside the scope of such a model.

1.3 Scope of the present paper

The purpose of the present paper is to present the results of some initial attempts at predicting the development of turbulent boundary layers in high accelerations. The prediction procedure employed is the finite-difference formulation of Patankar and Spalding (Ref.14) and the theoretical contribution of this work consists mainly of supplying preliminary turbulent shear-stress hypotheses to the Patankar-Spalding programme.

To aid the theoretical work, a more comprehensive experimental examination of similar sink-flow turbulent boundary layers has been started. Although this experimental work is far from complete, the results obtained to date were used to aid the selection of a provisional shear stress model for moderate accelerations.

As would be expected in a preliminary report, agreement between measurement and prediction is not perfect. The measure of agreement is, however, sufficiently good to lead one to expect that the reliable prediction of laminarisation is now an attainable objective.

2. Preliminary Models for Laminarisation

2.1 Moderate accelerations

2.1.1 Preliminary remarks

The findings of Refs.11 and 12, cited in Section 1.2 above, reveal that there is not a single critical value of K (or rather L) above which a normal turbulent boundary layer will degenerate to laminar. Rather, an acceleration will cause detectable changes in the structure of a turbulent boundary layer for values of K in excess of about 10^{-6} and these effects become more marked as K increases.

For a high enough acceleration, of course, it is known that a degeneration to laminar flow will ensue. This limit is probably in the neighbourhood of $K = 3 \times 10^{-6}$ and demarcates the upper value of what is meant by 'a moderate acceleration'. Before this limit is reached, however, a turbulent boundary layer will display marked departures from the 'universal' law of the wall.

The experiments of Refs.9 and 12 suggest that the principal changes that occur in a moderately-accelerated turbulent boundary layer take place in the sublayer; in crude terms, the region over which viscous stresses are significant becomes thicker (in terms of y^+). To a first approximation therefore, it would

seem/

seem plausible that, in moderate accelerations, laminarisation might be predicted by using an existing momentum-transport hypothesis for the main part of the layer provided some means was found of predicting the local thickness of the viscous sublayer.

It is in determining the thickness of the sublayer that the sink-flow boundary layers discussed in Section 1.2 are of great importance. For, since the boundary layers are similar, the sublayer thickness can be determined experimentally as a function of L^*. Having determined this relationship for similar boundary layers it might be thought that it would suffice for non-similar boundary layers as well. This is not, however, the case for it would imply that the local shear stress throughout the boundary layer was considerably affected by local conditions. Instead the authors have supposed that the rate at which the sublayer changes in thickness is linearly proportional to the 'amount' the sublayer is locally removed from its equilibrium condition. Of course a decision has to be made on how one is to quantify the above supposition. It will be seen that the choice made follows naturally from the form of effective viscosity hypothesis adopted in Section 2.1.2 below.

2.1.2 Choice of effective-viscosity input

Patankar and Spalding (Ref.14) illustrated the application of their finite-difference prediction procedure by using the Prandtl mixing-length hypothesis, with the following ramp distribution of mixing length, ℓ:

$$\tau = \rho \ell^2 \left(\frac{\partial u}{\partial y} \right) \left| \frac{\partial u}{\partial y} \right| \qquad \ldots (1)$$

$$\text{Inner region } \ell = ky \quad y \leq \frac{(\lambda y_L)}{k} \qquad \ldots (2a)$$

$$\text{Outer region } \ell = \lambda y_L \quad \frac{(\lambda y_L)}{k} < y \leq y_L \qquad \ldots (2b)$$

where y_L is the normal distance from the surface at which the velocity differs from the free-stream value by a small amount $f_R . U_G$; Patankar and Spalding chose $\lambda = 0.09$, $k = 0.435$ and $f_R = 0.01$.

The finite-difference solution was matched near the wall to the Couette-flow solutions calculated from a modified van Driest (Ref.15) expression for the variation of effective viscosity in the sublayer. Thus, the fluid viscosity did not appear explicitly in the finite difference equations. Reasonable agreement with experiment was achieved in a diversity of flow configurations. The chosen shear-stress model completely failed to predict the effects of laminarisation, however.

In the present work we need to specify a dependence of the effective viscosity in the sublayer on the laminarisation par-ter, L. For this reason, over the whole of the inner region the form of the effective viscosity distribution suggested by van Driest is adopted:

μ_{eff}/

*For sink-flow boundary layers, since K and c_f are constant, L is constant too.

$$\mu_{eff} = \mu + \rho(ky[1 - \exp(-y^+/A^+)])^2 \left|\frac{\partial u}{\partial y}\right| \quad \ldots (3)$$

Where

$$\mu_{eff} \equiv \tau / \left(\frac{\partial u}{\partial y}\right) .$$

The term A+ effectively determines the distance from the wall at which viscous shear stresses are significant, i.e., it may be interpreted as a sublayer thickness To fit existing pipe-flow data van Driest set A^+ equal to 26. In the present work A^+ for similar sink-flow boundary layers, is assumed to be a function of L. A provisional suggestion for $A^+_s(L)$ (where the 's' subscript denotes similar boundary Layers) is made in Section 2.1.3 below. For the present, k has been taken as 0.4, a frequently quoted value, rather than the value of 0.435 used by Patankar and Spalding.

For the outer region to the boundary layer, Patankar's mixing-length distribution is retained except that the mixing-length constant, λ, is multiplied by a matching function, M, to give continuity of shear stress at $y = (\lambda y_L/k)$. For values of K less than 2×10^{-6}, M differs negligibly from unity.

To summarize, the preliminary effective viscosity hypothesis for moderately accelerated turbulent boundary layers is:-

Inner region $\left(0 \leq y \leq \frac{\lambda y_L}{k}\right)$:

$$\mu_{eff} = \mu + \rho(ky[1 - \exp(-y^+/A^+)])^2 \left|\frac{\partial u}{\partial y}\right|$$

where $\lambda = .09$, $k = 0.40$ and A^+ is found from equations (5) and (6) below.

Outer region $\left(\frac{y_L}{k} < Y \leq y_L\right)$: ... (4)

$$\mu_{eff} = \rho(\lambda M y_L)^2 \left|\frac{\partial u}{\partial y}\right|$$

where M is chosen to give continuity of stear stress at

$$y = \frac{\lambda y_L}{k}$$

* In all the calculations reported herein, the value of the velocity-deficit fraction, f_R, at which y_L is determined is assigned the value .001.

2.1.3 The A^+_s (L) function

As stated above, the variation of A^+_s with the laminarisation parameter, L, is to be determined by reference to experimental measurements of similar sink-flow turbulent boundary layers. Unfortunately, the data of Launder and Stinchcombe (Ref.12) are not suitable for this purpose because the flow in their apparatus was not two-dimensional. The test section used in that study has been rebuilt, however, and to date one similar boundary layer has been set up and measured for a value of K of 2.2×10^{-6} (Jones (Ref.16)). Fig.3 compares the mean velocity distribution for this boundary layer with two theoretical velocity profiles; one for $A^+ = 61$. The latter value was chosen by trial and error so that the momentum-thickness Reynolds number was the same for the theoretical and the measured boundary layers. The experimental end theoretical profiles are inexoellent agreement all the way across the boundary layer. It is thus not surprising that the deduced c_f and H of 0.0048 and 1.51 should be accurately reproduced by the theoretical solution.

However, a single point is not sufficient to determine the complete A^+_s (L) function. When more data are available their implications till be incorporated; until then an interim hypothesis is needed. It is here assumed that, for Similar turbulent boundary layers, the viscous sublayer grows thicker as L is increased at a rate just sufficient to keep the skin friction coefficient constant. The value of c_f which these boundary layers are assumed to take on is that of the above experimental solution, i.e., 0.0048. The hypothesis implies that as L is increased from zero, A^+_s remains constant at its zero-pressure-gradient value of 26 until c_f has reached its maximum value. Thereafter, A^+_s increases to keep c_f constant.

Fig.4 shows the variation of A^+_s with L implied by the above hypothesis. From the theoretical solutions A", varies nearly linearly with L and so, for simplicity, the A^+_s (L) given by the solid line on Fig.4 is chosen; it is:

$$A^+_s = 26 \qquad L \leq 1.9 \times 10^{-3}$$

$$A^+_s = 11 + (7.9 \times 10^3)L; \; L > 1.9 \times 10^{-3} \qquad \ldots \quad (5)$$

Figs.5 and 6 compare the experimental and theoretical variation of R_2 and H with K for sink-flow turbulent boundary layers. The Reynolds-number data of Ref.12 lie rather below the prediction obtained with equation (5). As remarked above, this discrepancy is attributable to the slight three-dimensionality of the flow. The shape factor, as would be expected, is in better agreement.

Generally, the chosen A^+_s (L) function displays the desired approach of the turbulent boundary-layer solutions to the laminar solution of Pohlhausen (Ref.17) as the K is increased, and would suggest that the assumption of a constant c_f was not far removed from the truth.

2.1.4 A+ in non-similar boundary layers

Following the remarks in Section 2.1.1, the variations of A" with respect to x in non-similar boundary layers is determined from the equation:

$$\frac{dA^+}{ax+} = c\,(A^+_s - A+) \qquad \ldots \quad (6)$$

where/

where A^+_s is here the similar value of A+ corresponding to the local value of L; it is determined by equation (5). The constant c has to be determined empirically and a provisional recommendation is made in Section 3.

2.2 'Severe' accelerations

For moderate accelerations it has been assumed that the only effect of the acceleration on the structure of the turbulent boundary layer was in the growth of the viscous sub-layer. Outside of the sub-layer the mixing-length formulation for the transfer of momentum and heat were assumed to be virtually the same as for other types of turbulent boundary layer.

While such assumptions may lead to useful predictions for moderate accelerations, they must be a very long way from the truth in 'severe' accelerations - say, for $X > 10^{-5}$.

For such flows, a more reasonable guess would be that the shear stress along a stream-line remained constant. This assumption neglects entirely the effects of diffusion, dissipation and production. The implicit assumption is that the fluid within the boundary layer is accelerated so quickly that there is not time for these terms to change the turbulent shear stress appreciably. Launder (Ref.9) has made hot wire measurements of severely accelerated boundary layers ($K_{max} \approx 1.5 \times 10^{-5}$) and has found that over the outer part of the boundary layer, $\overline{u'v'}$ was virtually constant along a streamline. Near the wall, the assumption is not a good one and the current specifications will soon be superseded.

The above model has also been incorporated into the Patankar-Spalding programme; comparison of prediction with a limited amount of data is made in the following section.

2.3 The effective-Prandtl-number-specification

The present framework of the Patankar-Spalding prediction procedure required the effective Prandtl/Schmidt number, σ_{eff}, to be specified for the calculation of dependent variables other than u. For the present, the assumption used by Patankar and Spalding is retained. By definition the effective Prandtl number may be expressed:

$$\frac{\mu_{eff}}{\sigma_{eff}} = \frac{\mu}{\sigma} + \frac{(\mu_{eff} - \mu)}{\sigma_t} \qquad \ldots (7)$$

where σ_t is the turbulent Prandtl number. σ_t is here assigned the value 0.90 throughout the boundary layer.

2.4 Modifications to the Patankar-Spalding computer programme

There mere two principal changes made to the existing version of the Patankar-Spalding finite-difference computer programme. Firstly, new subroutines VEFF were written to incorporate the two-effective viscosity models discussed above.

Secondly, since the changes in structure of a turbulent boundary layer undergoing laminarisation appeared first in the sublayer, the finite-difference calculations were carried close enough to the wall for the solution to be matched to the laminar boundary conditions:

u^+/

$$u^+ = y^+ + p_+ Y^{+2}/2; \quad t^+ = \sigma y^+ \qquad \ldots (8)$$

at a y^+ of about 1. Subroutines WALL, WF1 and WF2 were modified appropriately.

Further, since finite-difference calculations wre to be made in the viscous sublayer where the curvature of the velocity and temperature profiles were large (with ω as independent variable), the grid. spacing near the wall had to be small, All the DIMENSION statements in the programme were thus modified to allow for up to 100 grid points across the boundary layer.

3. Comparison with Experiment

3.1 Constant turbulent shear stress along a streamline

Figs.7 and 8 show the variations of R_2 and H in two of Launder's (Ref.9) experiments. The shape of the nozzle (shown in Fig.1) caused the acceleration parameter, K, to rise rapidly over a length of about 6 inches and then to fall even more rapidly towards zero. The theoretical solution? computed by the Patankar-Spalding finite-difference procedure with the constant-?? model are shown in these figures by a broken line.

The largest values of K are attained in the test shown in Fig.7 and it is these data which we should expect the constant-m model to predict most accurately; this, indeed, proves to be the case. The measured variation of shape factor is faithfully reproduced by the prediction; in particular, the fact that much of the increase in shape factor occurs well downstream of the peak in the K curve. The theoretical momentum thickness Reynolds number is less than the measured ones over the region where K is greatest. The overall agreement, however, is reasonably satisfactory.

For the test shown in Fig.8, in which the maximum value of K was about 8×10^{-6}, the shape factor variation is likewise well-predicted. The theoretical variation of H does not display the measured sharp decrease someway downstream from the acceleration but this is entirely to be expected since the theoretical model for shear stress contains no means by which a laminarised boundary layer can subsequently undergo retransition to turbulent. The variation of R_2 through the acceleration is not predicted very accurately and this may, in part, be due to starting the computation at a data point where the measured momentum thickness would appear to be spuriously low.

Taking the above results as a whole, it is concluded that the assumption that the turbulent shear stress is constant along a stream line can lead to reasonably accurate predictions of laminarisation in severe accelerations. And the above comparisons with data suggest that the value proposed in Section 2, $K = 10^{-5}$, is a reasonable rule of thumb to decide whether or not an acceleration can be treated as severe.

3.2 The A" *model*

Examples of the successes and shortcomings of the A^+-model described in Section 2.1.4 is provided in Figs.9 - 11. Fig.9 shows the predictions obtained with the Patankar-Spalding programme of the Filetti data shown previously in Fig.2. The empirical constant 'c' appearing in equation (6) was chosen such that the agreement with the data is as good possible. Indeed, two values of c were selected; for $A^+ \leq A^+_s$, c was assigned the value of 10^{-4}; for $A^+ > A^+_s$, c was set equal 5.0×10^{-4}. Agreement is *impressive* but the result is not surprising since this set of data has been taken as the basis for choosing c.

Figs./

Figs.10 and 11 display comparisons between data of Filetti's Run 2 and Moretti and Kays' Run 11 in which c is assigned the values quoted above. It is seen in Fig.10 that the predicted and measured Stanton numbers for Filetti's Run 2 are again in excellent agreement. The result is not remarkable for again the acceleration was such that, in the accelerating region, K was virtually uniform, i.e., the type of acceleration was similar to that shown in Fig.9 from which the values of 0 were chosen.

In Fig.11 it is seen that the Moretti and Kays data are not well predicted by the present model. The fundamental defect is that the model predicts a rapid rise in Stanton number at the start of the acceleration which is not borne out by the measurements. As a result, even though the predicted Stanton number subsequently falls rapidly, the predicted minimum value is about 80% higher than the measured.

It was initially suspected that the predicted rise in Stanton number was due to mathematical inaccuracies in performing the computations which were attributable in sane way to extending the finite-difference calculations to the immediate vicinity of the surface. This suspicionwss reinforced by the fact that Patamkar and Spalding, who matched the finite-differenoe solution to wall functions outside of the viscous region, had not predicted any rise in Stanton number at the start of an acceleration. Reductions in the size of forward step and redistribution of grid lines, however, did not lead to any appreciable change in the predictions. Moreover, the fact that the integral conservation equations were closely satisfied further implied that a mathematically accurate solution of the partial differential equations was being obtained - the shortcomings of the predictions was thus attributable to the imperfections of the model.

It was eventually discovered that the sudden rise in Stanton number could be eliminated if the local-stress, τ, rather than the wall shear stress τ_w was used in the exponential term of equation (3);

that is:

$$\mu_{eff} = \mu + \rho(ky[1 - \exp(-\sqrt{\frac{\tau}{\rho}}/A^+)])^2 \left|\frac{\partial u}{\partial y}\right| \qquad \ldots (9)$$

The dotted line in Fig.11 clearly shows the improved predictions which result from the use of equation (9) rather than (3).

4. Conclusions and Concluding Remarks.

(i) In severe accelerations ($K > 10^{-5}$), the assumption that the turbulent shear stress remains constant along a streamline has led to reasonably accurate predictions of R_2 and H.

(ii) For moderate accelerations, a model has been proposed which makes use of the Prandtl mixing-length formula for effective viscosity and the van Driest proposal for the variation of mixing length near the wall. However the 'damping' function A^+ (which van Driest chose to be a constant-equal to 26) is a variable whose value is found from the solution of an ordinary differential equation (equation(6)). In an aooelerating flow, A^+ mill. exceed its zero-pressure-gradient value and this effectively increases the thickness of the viscous sublayer. A consequence is that the Stanton number decreases rapidly.

Comparisons/

Comparisons with data have shown that the model may well be capable of providing a useful indication of the level of wall heat-transfer rates which are likely to prevail in moderate accelerations. Further development and testing is currently in progress.

(iii) A major shortcoming of a model such as that described in the above paragraph is that it is a long way removed from the essential physics of the laminarisation process. For the future, a more reliable basis for prediction will undoubtedly entail the solution of additional partial differential equations which describe the development of properties of the turbulent flow field (e.g., the turbulent kinetic energy, the turbulent length scale). However, to establish and refine such solution procedures will take a year or two yet. In the meantime, the A^{+}-model provides a means of predicting laminarisation with a fair degree of accuracy.

5. Nomenclature

A^+ a function appearing in the van Driest formula for effective viscosity.

A^+_s A^+ in a similar boundary layer.

c an empirical constant (equation (6)).

c_f skin friction coefficient $\dfrac{\tau_w}{\frac{1}{2}\rho U_G^2}$.

f_R value of normalised velocity deficit at which y_L is determined.

H shape factor δ_1/δ_2.

k von Karman constant (0.40).

K acceleration parameter $\dfrac{\nu}{U_G^2}\dfrac{dU_G}{dx}$.

L laminarisation parameter $Kc_f^{-3/2}$.

M matching function (equation (4)).

p_+ dimensionless pressure gradient $\dfrac{\nu}{\rho u_\tau^3}\dfrac{dp}{dx}$.

R_2 momentum thickness Reynolds number $\dfrac{\delta_2 U_G}{\nu}$.

u local mean velocity parallel to wall.

u_τ friction velocity $(\tau_w/\rho)^{\frac{1}{2}}$.

U_G local free stream velocity.

y Cartesian co-ordinate normal to wall.

y^+ dimensionless value of y: $u_\tau y/\nu$.

y_G value of y at edge of boundary layer.

y_L value of y for calculation of value of mixing length for outer part of boundary layer.

x Cartesian co-ordinate in the mean flow direction.

a dimensionless value of x: $u_\tau x/\nu$.

δ_1 displacement thickness $\displaystyle\int_0^\infty (1 - u/U_G)\, dy$.

δ_2 momentum-deficit thickness $\displaystyle\int_0^\infty \frac{u}{U_G}\left(1 - \frac{u}{U_G}\right) dy$.

λ dimensionless value of Prandtl mixing length (0.09).

μ molecular dynamic viscosity.

μ_{eff} effective (total) dynamic viscosity of fluid in turbulent flow: $\frac{\tau}{(\partial u/\partial y)}$

ν molecular kinematic viscosity,

ρ fluid density.

τ total (turbulent + laminar) sheer stress.

τ_w wall shear stress.

ω dimensionless stream function; independent cross-stream variable in Patankar-Spalding procedure.

References/

References

No.	Author(s)	Title, etc.
1	Y. Senoo	The boundary layer on the end wall of a turbine nozzle cascade.- Trans. ASME 80, p.1711.
2	J. Sternberg	The transition from a turbulent to a laminar boundary layer.- US Army Bal. Res. Lab. Rept.906, Aberdeen, May, 1954.
3	A. A. Sergienko and V. K. Gretsov	Transition from a turbulent into a laminar boundary layer.- Soviet Physics Doklady 4, 2 (Oct. 1959), p.275.
4	B. H. Back, P. F. Massier and H. L. Ger	Convecting heat-transfer in a convective-divergent nozzle.- Int. J. Heat and Mass Transfer 7, 5 (May 1964), p.549.
5	B. E. Launder	Laminarisation of the turbulent boundary layer in a severe acceleration.- J. App. Mech. Vol. 31 (Dec. 1964), p.707.
6	V. C. Patel	Calibration of the Preston tube and limitations on its use in pressure gradient.- J. Fluid Mech. 23 p.185, 1965.
7	E. G. Filetti	University of Stanford unpublished report. Data quoted by Moretti and Xays (Ref.10).
8	Z. Zario	Turbulent heat transfer in a divergent-convergent channel.- JSME 1967, Semi-Int. Sym. Tokyo.
9	B. E. Launder	Laminarisation of the turbulent boundary layer by acceleration.- MIT Gas Turbine Lab. Report No.77.
10	P. M. Moretti and W. M. Kays	Heat transfer through an incompressible turbulent boundary layer with varying free-stream velocity and varying surface temperature.- Stanford University, Mech. Eng. Dept. Report No. PG-1.
11	F. A. Schraub and S. J. Kline	A study of the structure of the turbulent boundary layer with and without longitudinal pressure gradients.- Thermosci. Div. Report MD-12, Stanford University 1965.
12	B. E. Launder and H. S. Stinchcombe	Non-normal similar turbulent boundary layers.- Imperial College, Mech. Eng. Dept., TWF/TN/21, 1967.
13	R. Parkinson	Convective heat transfer in rocket engines. Part II: Heat transfer to the nozzle.- Unpublished Mintech Report.

References

No.	Author(s)	Title, etc.
14	D. B. Spalding and S. V. Patankar	Heat and mass transfer in boundary layers.- Pub. by Morgan-Grampian Books Ltd. 1967.
15	E. R. van Driest	On turbulent flow near a wall.- J. Aero. Sci. 23, 1956, p.1007.
16	W. P. Jones	Strongly accelerated turbulent boundary lagers.- M.Sc. Thesis, Imperial College, 1967.
17	K. Pohlhausen	Zur näherungsweisen Integration der Differentialgleichung der laminaren Grenzschicht.- Z. angew. Math. Mech. vol.1, p.252, 1921.
18	H. J. Herring and J. F. Norbury	Some experiments on equilibrium turbulent boundary layers in favourable pressure gradient.- J. Fluid Mech. 27 p.541, 1967.

EM

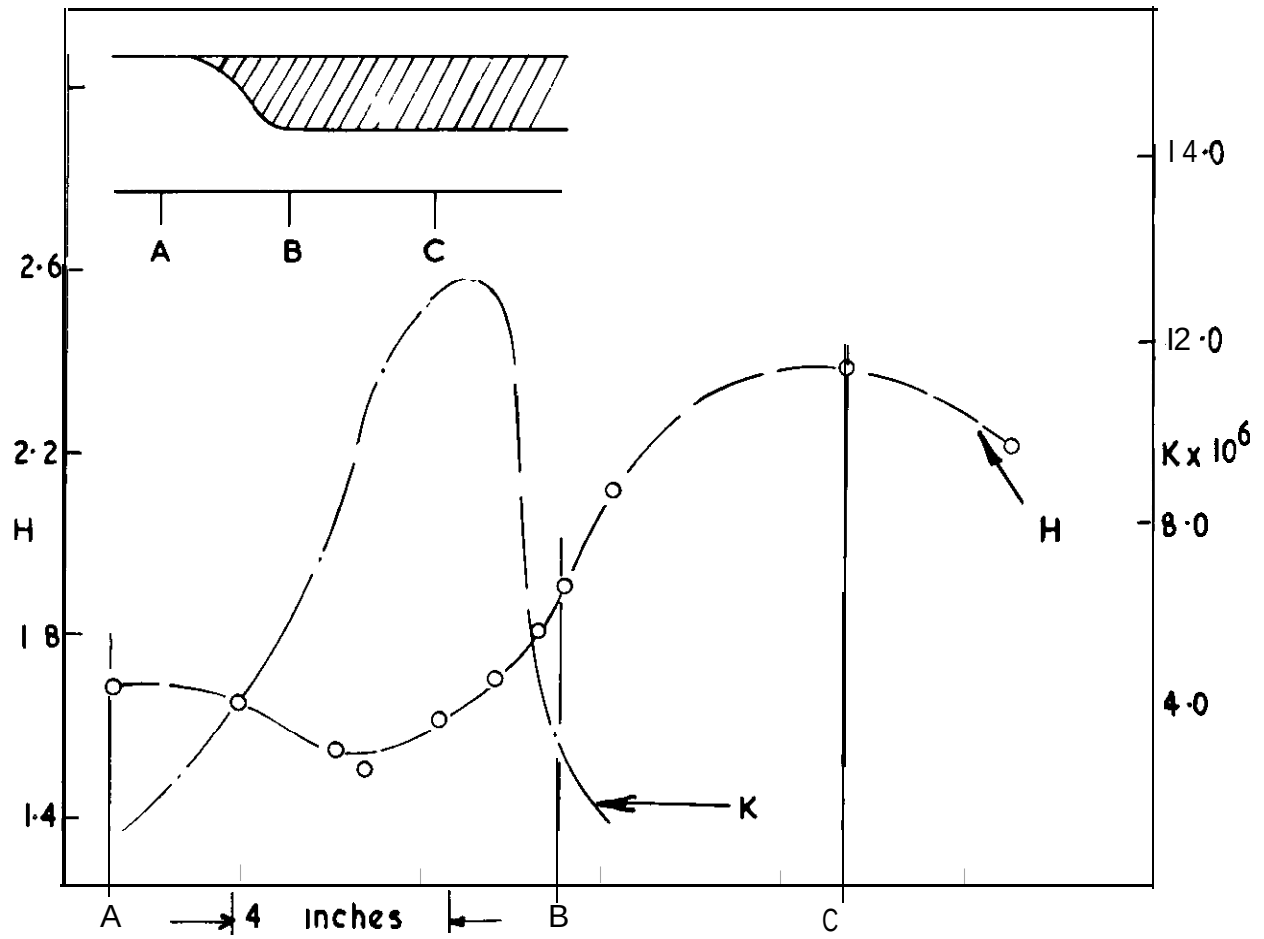

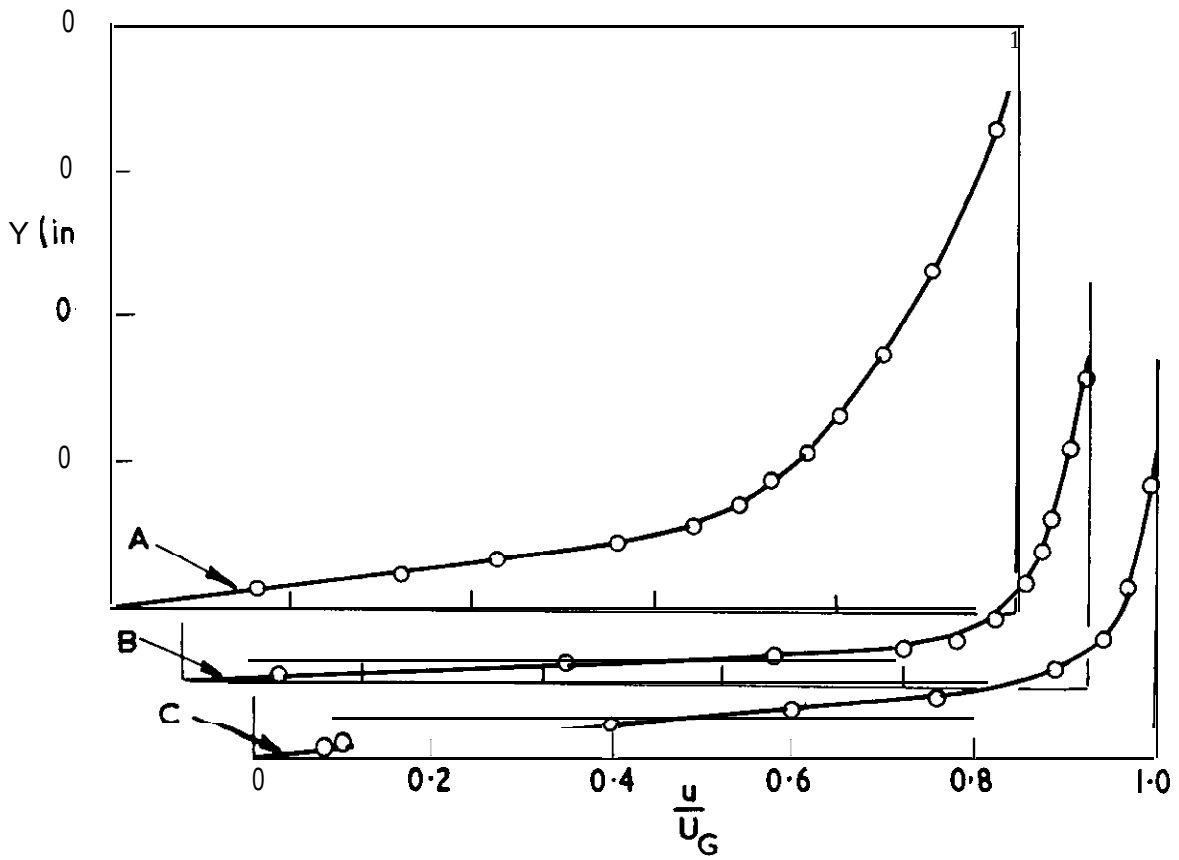

FIG. 1 Shape factor and velocity profiles in severe acceleration (Launder (9))

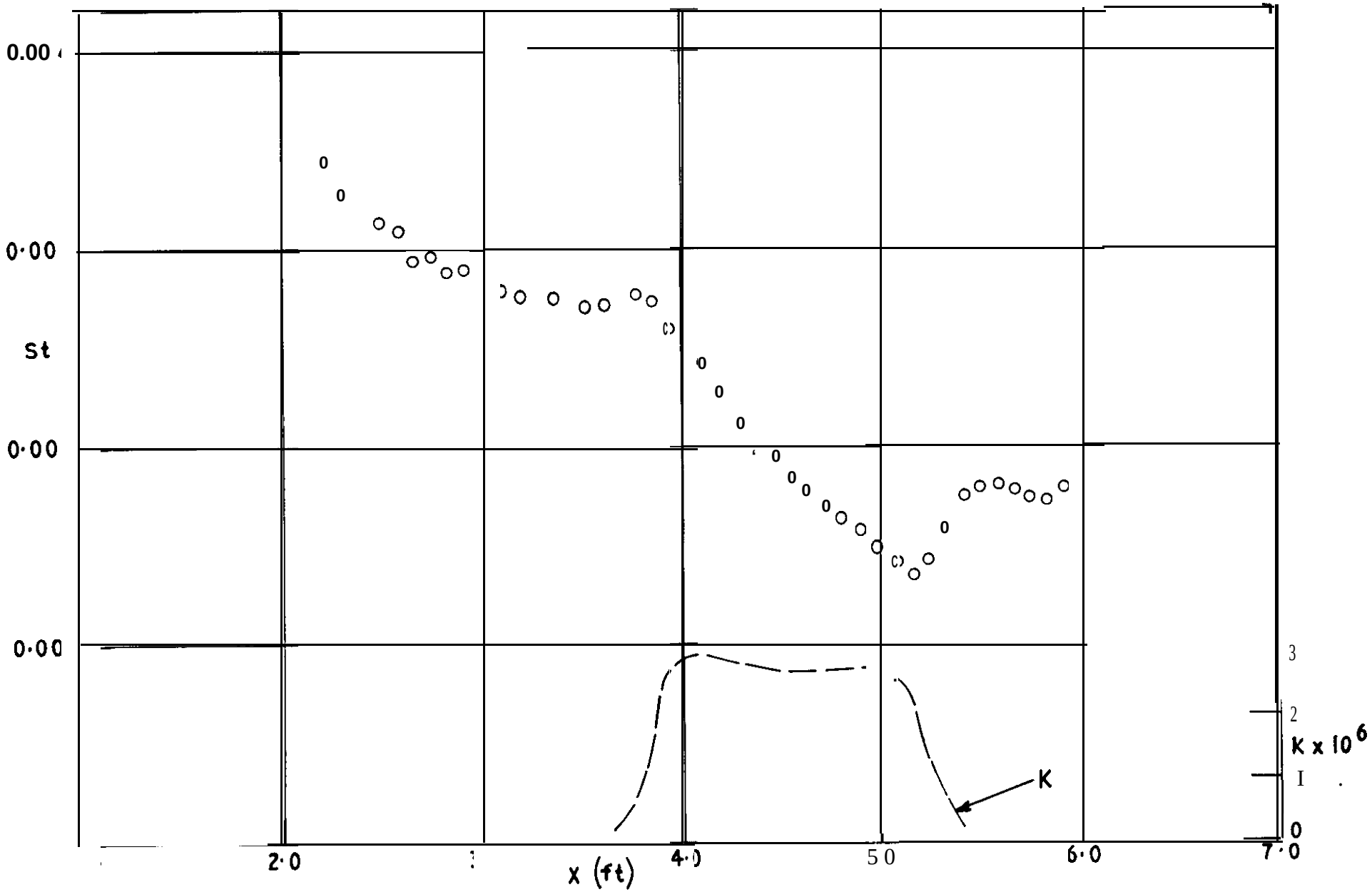

FIG.2 St vs X Data of Filettl (7)

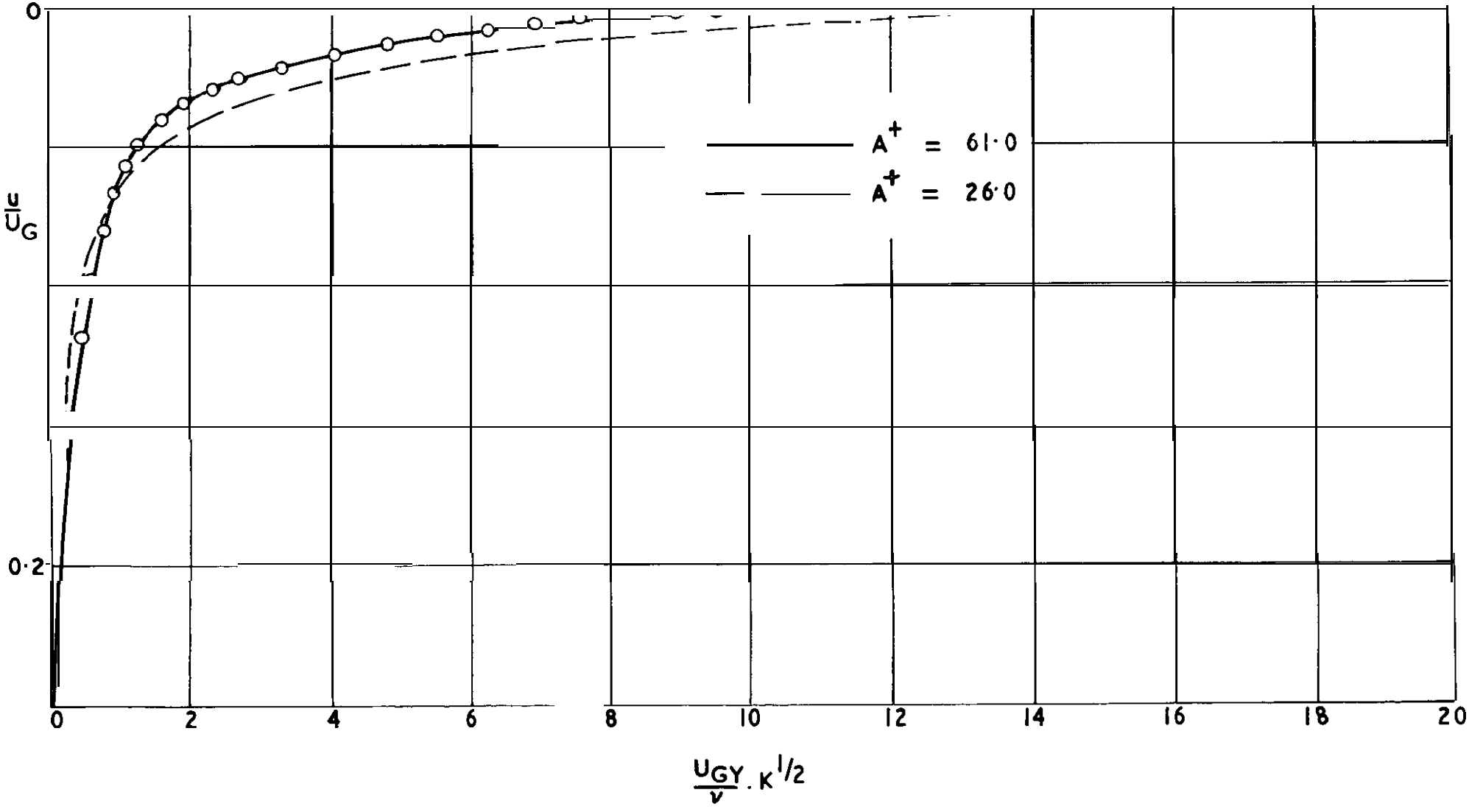

FIG 3 Experimental theoretical solution to sink-flow boundary layer $K = 2{\cdot}2 \times 10^{-6}$ (Jones (16))

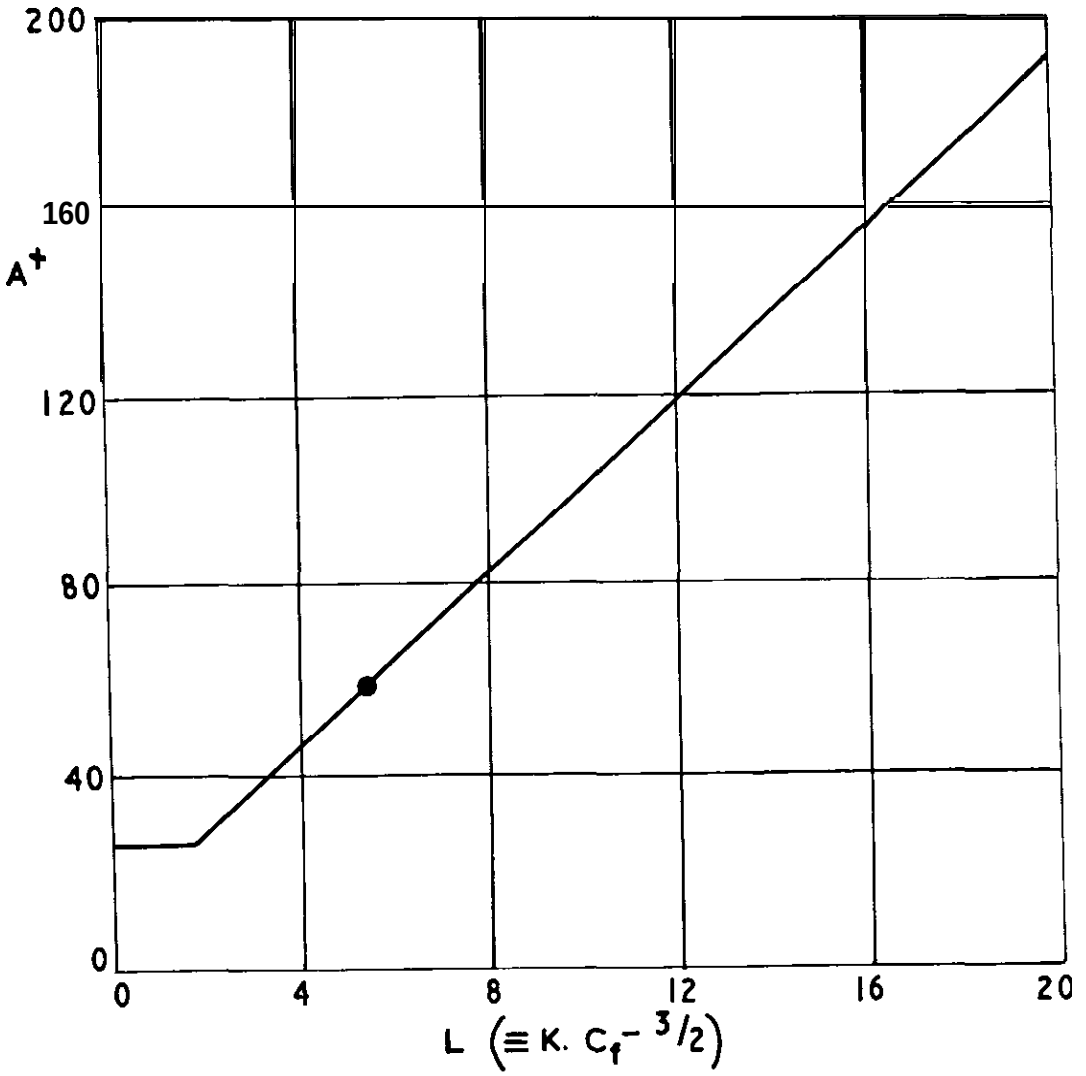

FIG.4 Provisional A+(L) relationship for sink-flow boundary layers

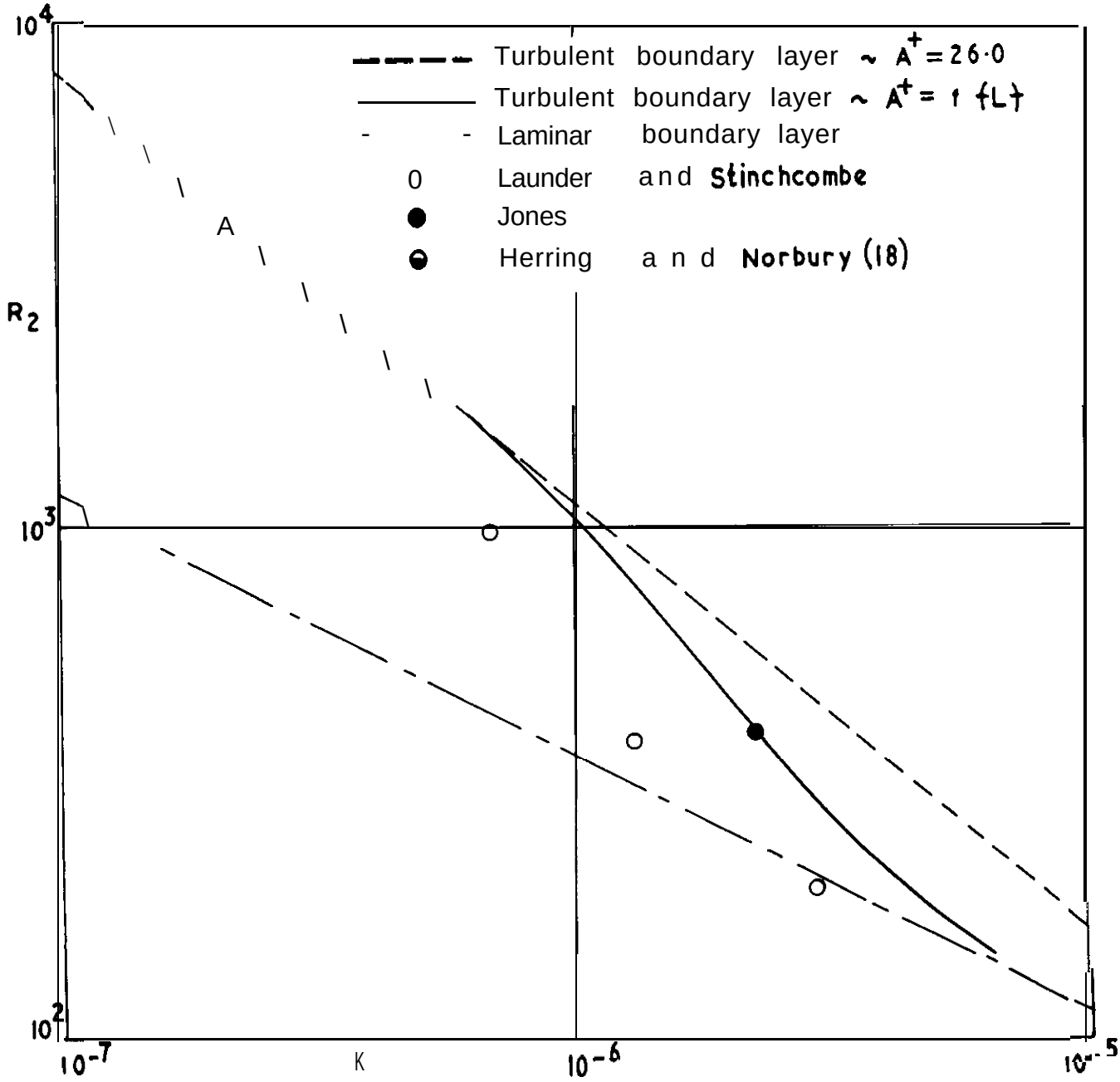

FIG. 5 R_2 vs K. Relations tor smk-flow boundary layers

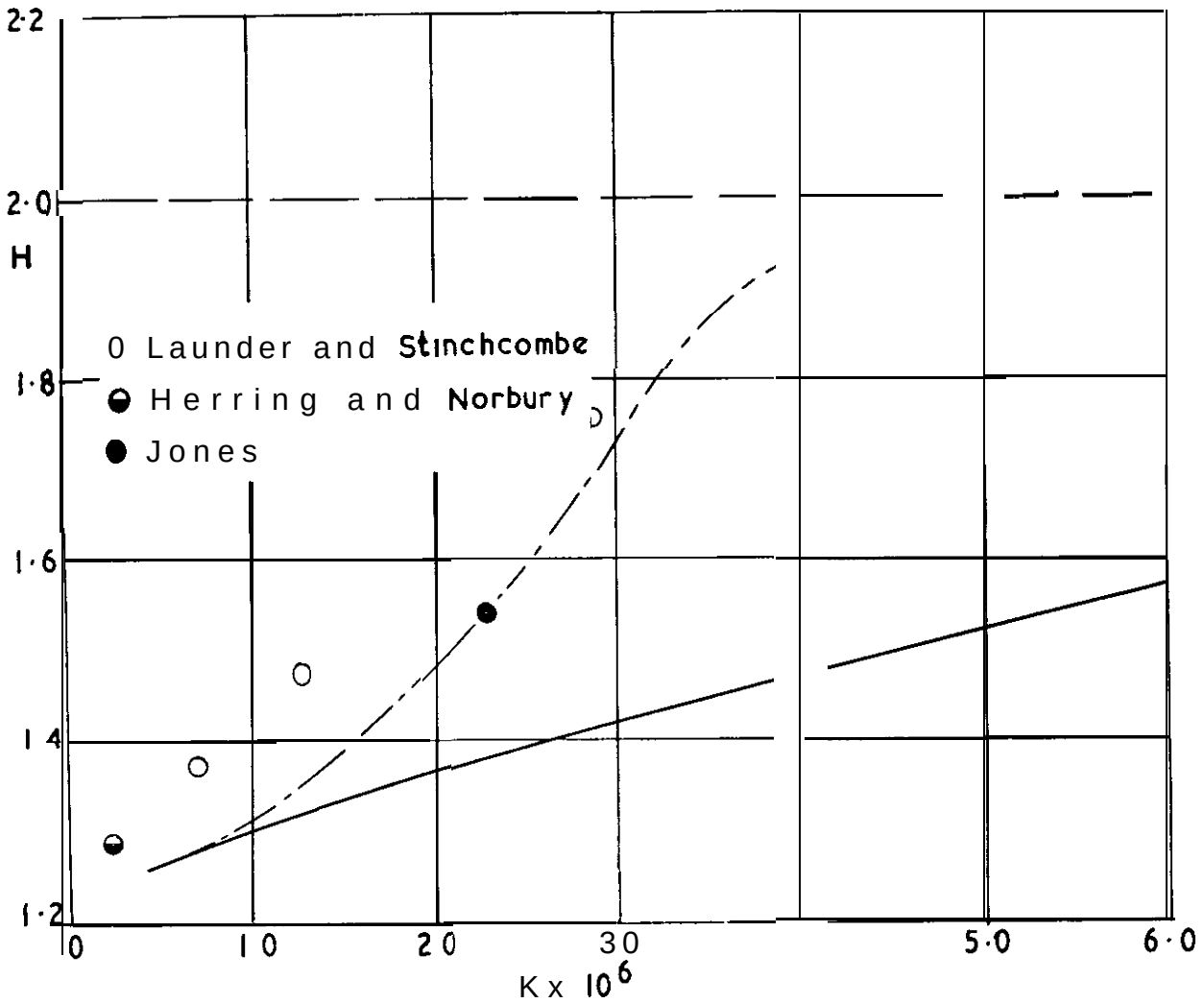

FIG 6 **H vs** K Relations for sink-flow boundary layers

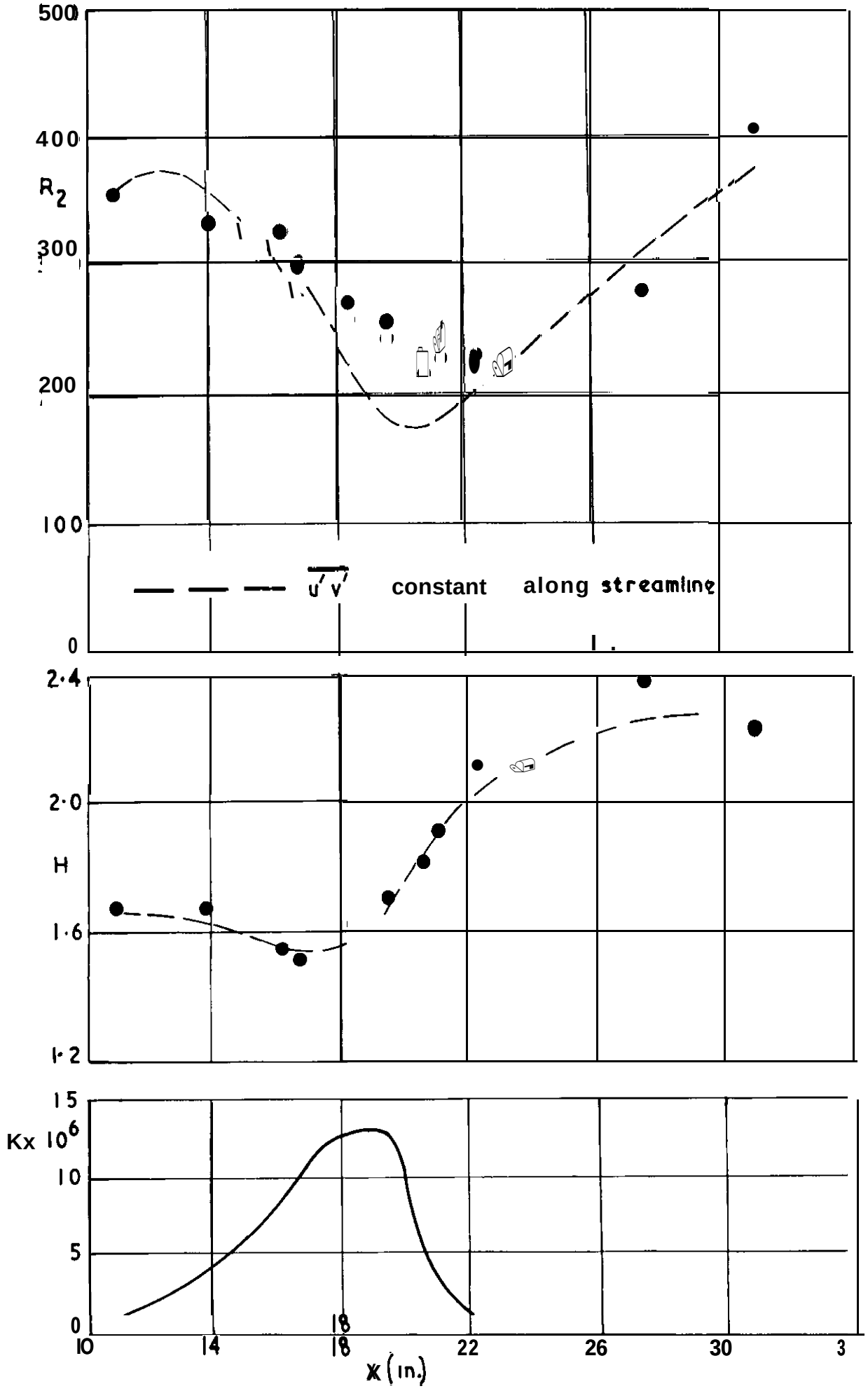

FIG.7 R_2 and H vs X. Data of Launder

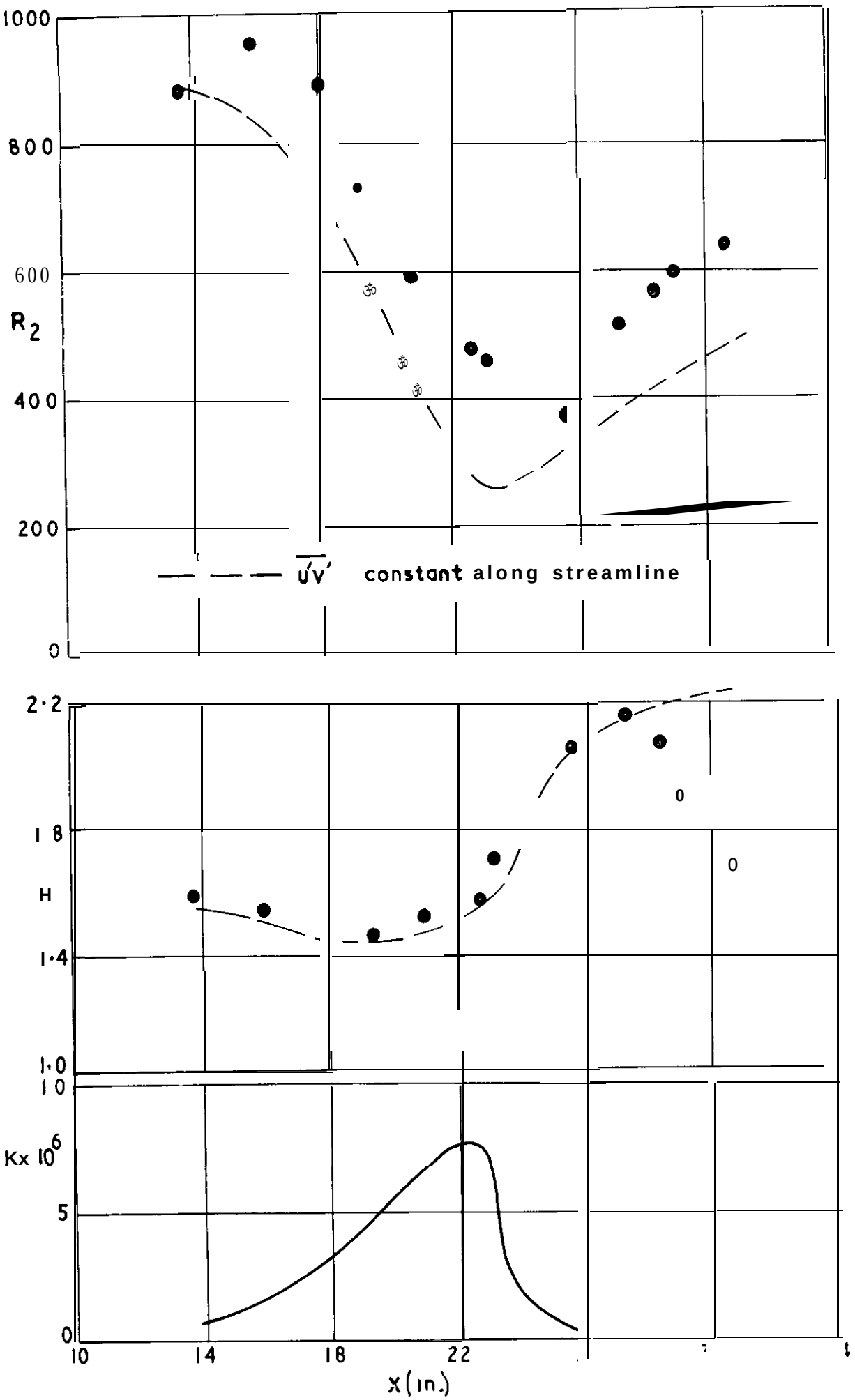

FIG 8 R_2 and H vs X. Data of Launder

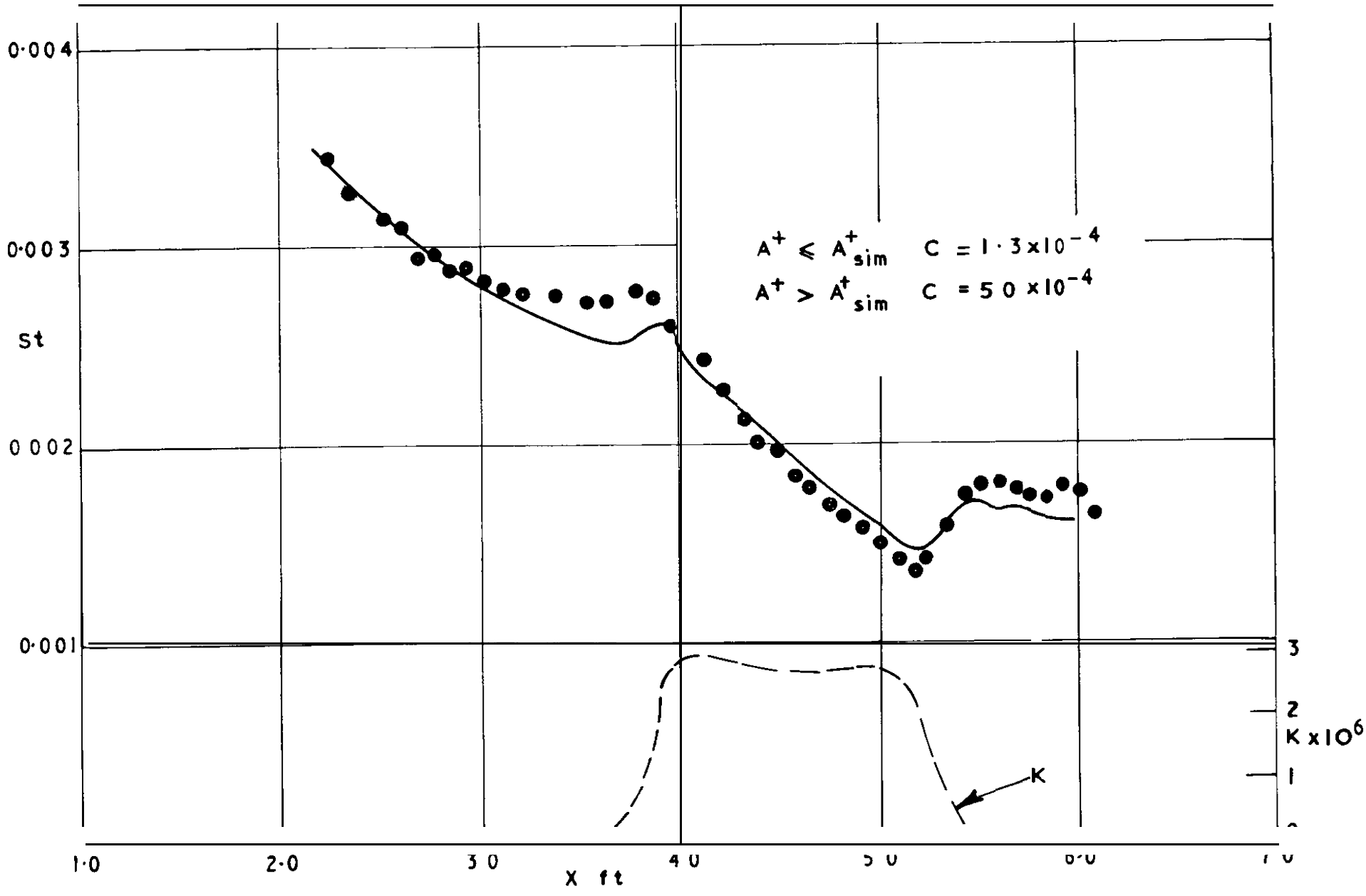

FIG 9 St vs X Data of Filetti-run 2

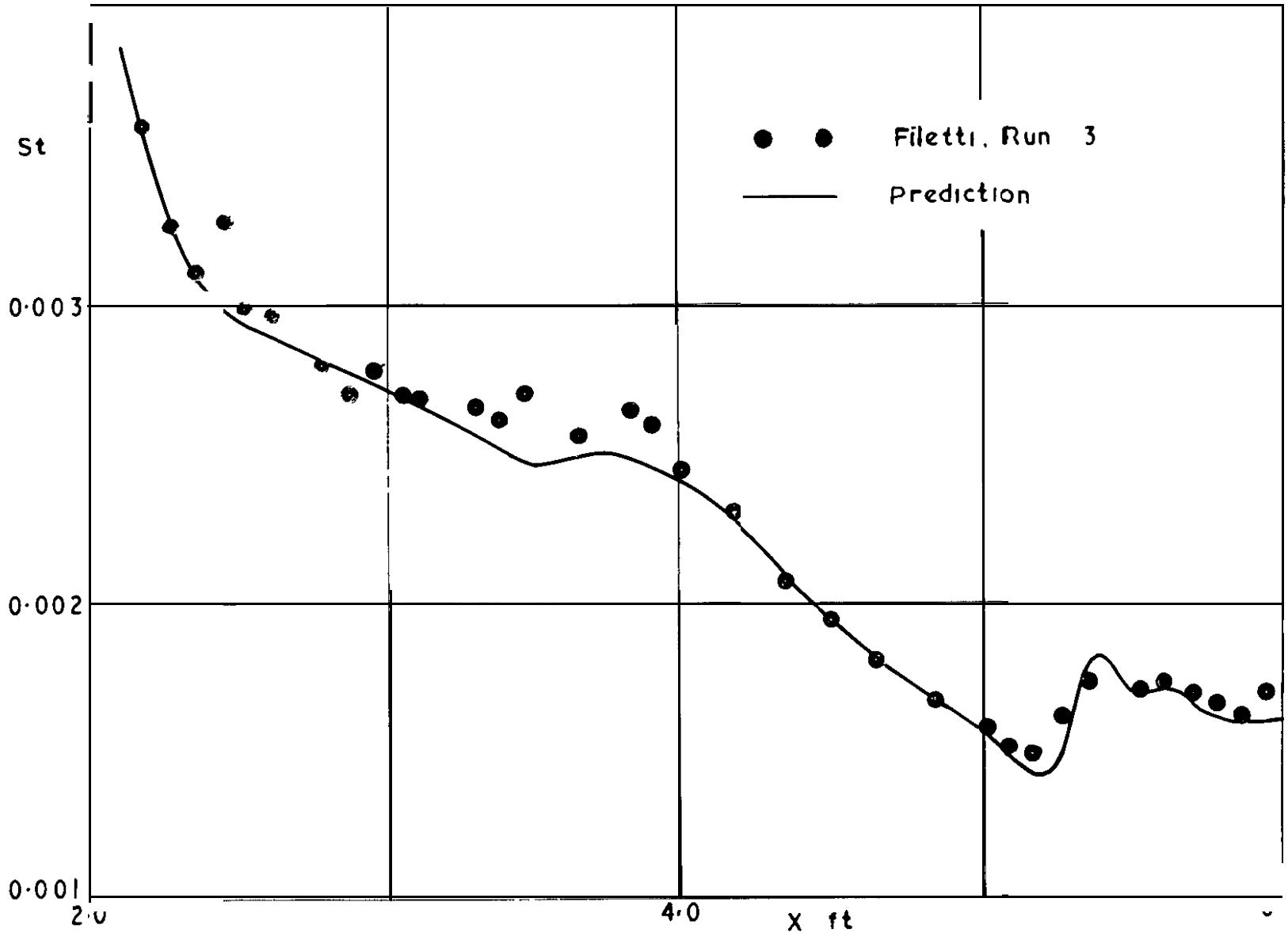

FIG 10 St vs X Data of Filetti

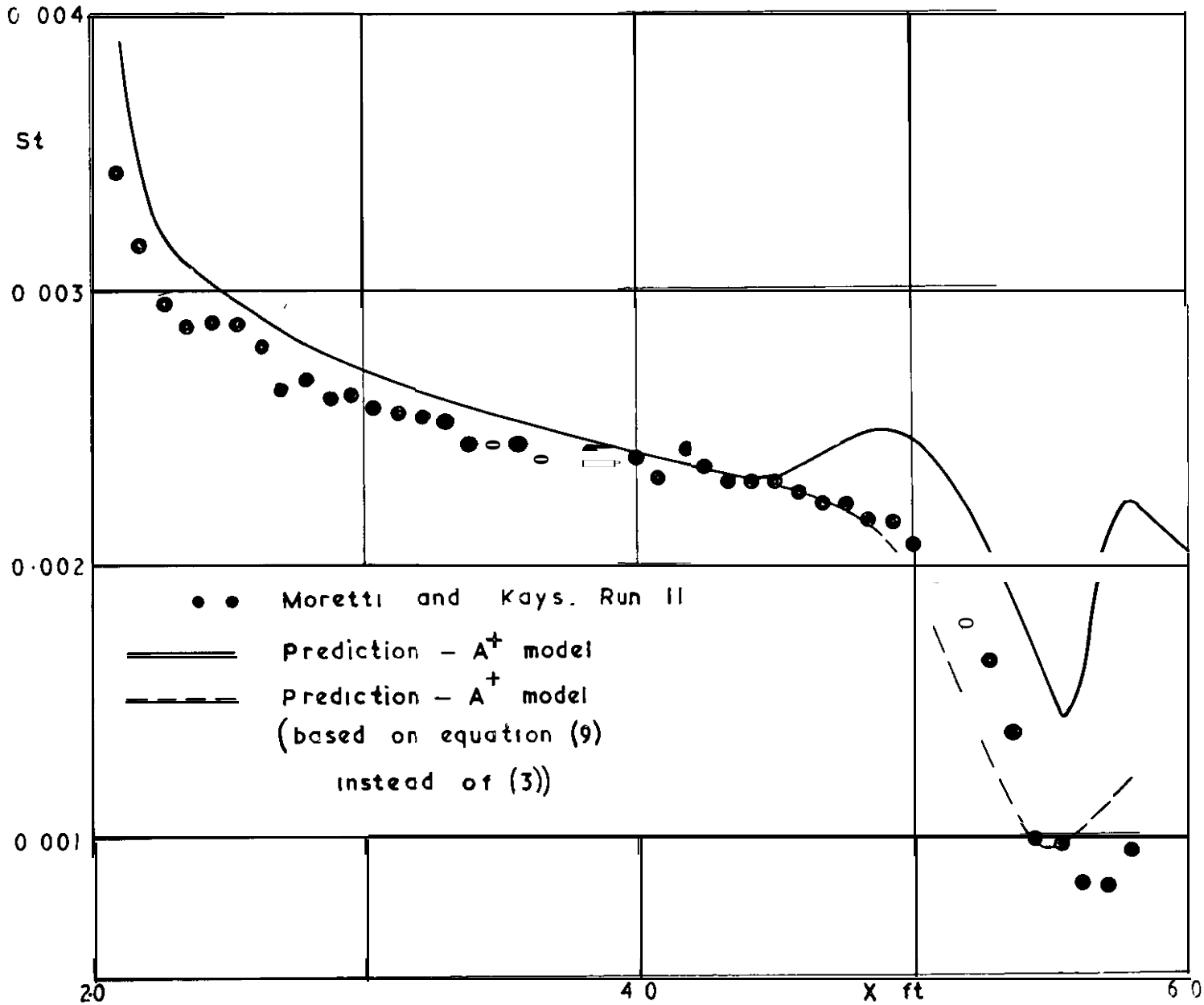

FIG 11 St vs X. Comparison of predicted variation with data of Moretti and Kays

Printed and published by
HER MAJESTY'S STATIONERY OFFICE

To be purchased from
49 High Holborn, London W C 1
13A Castle Street, Edinburgh 2
109 St Mary Street, Cardiff CF1 1JW
Brazennose Street, Manchester M60 8AS
50 Fairfax Street, Bristol BS1 3DE
258 Broad Street, Birmingham 1
7 Linenhall Street, Belfast BT2 8AY
or through any bookseller

Printed in England

SBN 1, 470163 6